

# Nanoscopic time crystal obtained by non-ergodic spin dynamics

Carla Lupo<sup>1</sup> and Cedric Weber<sup>1</sup>

<sup>1</sup>*King's College London, Theory and Simulation of Condensed Matter, The Strand, WC2R 2LS London, UK*

(Dated: December 14, 2024)

We study the far-from-equilibrium properties of quenched magnetic nanoscopic classical spin systems. In particular, we focus on the interplay between lattice vibrations and magnetic frustrations induced by surface effects typical of an antiferromagnet. We use a combination of Monte Carlo simulations and explore the dynamical behaviours by solving the stochastic Landau-Lifshitz-Gilbert equation at finite temperature. The Monte Carlo approach treats both the ionic degrees of freedom and spin variables on the same footing, via an extended Lennard-Jones Hamiltonian with a spin-lattice coupling. The zero temperature phase diagram of the finite size nanoscopic systems with respect to the range of the Heisenberg interaction and the Lennard-Jones coupling constant shows two main structures with non-trivial magnetisation triggered by antiferromagnetism: a simple cubic and a body-centred cubic. At non zero temperature, the competition between spins and the ionic vibrations considerably affects the magnetization of the system. Exploring the dynamics reveals a non-trivial structural induced behaviour in the spin relaxation with a concomitant memory of the initially applied ferromagnetic quench. We report the observation of a non-trivial dynamical scenario, obtained after a ferromagnetic magnetic quench at low temperature. Furthermore, we observe long-lived non-thermal states which could open new avenues for nano-technology.

Many-body systems comprise a wide range of systems, from simple metals, organic molecules, all the way up to cells. While their physics can be extremely rich, this complexity is however often irrelevant, as such systems will typically - at equilibrium - thermalise, a process through which most information about their preparation history and their initial state is lost [1, 2]. This behaviour is typical for ergodic systems in the thermodynamic limit and allows to calculate physical observables and make predictions that can be measured and tested. However, ergodicity can be broken out-of-equilibrium [3], in particular by inducing non-thermal states that keep a memory of their initial condition for long times. Those peculiar behaviours have been explored in novel non-equilibrium phases of matter, which includes Floquet symmetry protected topological phases [4] and time crystals [5, 6]. While bulk systems have been extensively investigated, nanoscopic systems remain open to questions. Recent progress in nano-engineering and the design of nanoscopic systems, such as nano-magnets made of single atoms arrays as memory devices [7], has opened new possibilities to explore quantum states in systems where thermalisation is not obtained, in particular for quenched and periodically-driven systems. Indeed, it has been observed that finite size effects allow these systems to keep a much better local memory of their initial conditions [8]. Experimental advances in manipulation and switching of the magnetization - possible even at the femtosecond level [9]- have triggered new studies in spin dynamics towards the microscopic understanding of the emerging relaxation time scales in nanoscopic systems. Particular attention has been paid to cases where antiferromagnetic order is involved [10, 11] : in these systems the contribution of the uncompensated spins at the surface trigger exotic phenomena which are not analytically tractable and whose

precise understanding is still unknown. To that end, new mechanisms for slow relaxation and non-ergodicity might have potential implications for the design and control of novel quantum non-equilibrium materials and devices. In this work, we propose a study of the dynamics of a typical many-body nanoscopic system in which the relaxation processes involve both the structure and magnetic moments. As describing the time evolution of quantum coupled magnetic moments and ions is beyond the reach of current state-of-the-art approaches, we will consider in this work the quenched and driven classical spins, in the presence of long-range magnetic interactions coupled to the lattice dynamics. We first focus on the interplay of the local ordered magnetic moments and the lattice dynamics at finite temperature. This provides a structural phase diagram, where the ordered phase is characterized. Next, we extend the equilibrium calculations to a ferromagnetic quench. We go on to study the equilibrium and out of equilibrium properties using a combination of Monte Carlo simulations - already widely applied in the characterization of bulk systems [12, 13] - and atomistic spin dynamics, [14, 15], respectively. The dynamics are explored through the numerical implementation of the Landau-Lifshitz-Gilbert [16] equation extended to deal with finite temperatures within a Langevin dynamics framework. We demonstrate slow relaxation and possible non-ergodicity in non-disordered nanoscopic many-body systems through the magnetic quench of typical nano-particle systems.

*Equilibrium Properties: Spin-Lattice Hamiltonian*  
We consider a cluster in a spherical shape with radius  $R$  and simple cubic structure (SC) with unitary lattice constant. The total lattice-spin Hamiltonian of the clus-

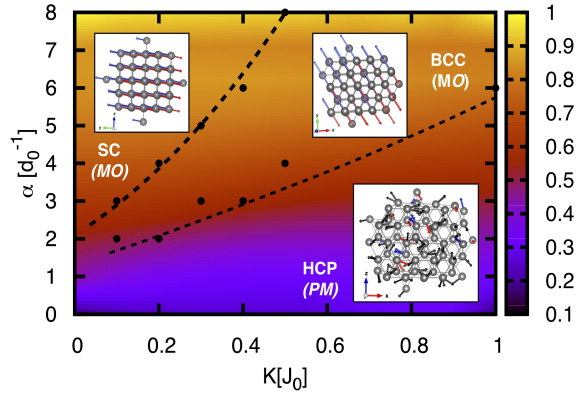


Figure 1: (colors online) Zero temperature structural phase diagrams with respect to the interaction range  $\alpha$  and the Lennard Jones potential  $K$ . Dashed lines are guides to the eyes and distinguish three different structural regions characterized by the following geometries: simple cubic (SC), body-centered-cubic (BCC) and hexagonal-closed packed (HCP). Shaded colours indicate the presence of antiferromagnetic order (MO). The arrows represent one possible spin configuration for the collinear magnetic order (at  $\mathbf{Q} = (\pi, \pi, \pi)/a$  for SC and  $\mathbf{Q} = (0, 0, 2\pi)/a$ ) and magnetic disorder for the HCP. The size of the system in analysis is 123 sites.

ter reads as follows:

$$H(\mathbf{S}_i, \mathbf{S}_j, d_{ij}) = - \sum_{i,j} J(d_{ij}) \mathbf{S}_i \cdot \mathbf{S}_j + K \sum_{i,j} \left[ \left( \frac{d^0}{d_{ij}} \right)^{12} - 2 \left( \frac{d^0}{d_{ij}} \right)^6 \right] \quad (1)$$

where  $\mathbf{S}_i$  are  $O(3)$  unitary  $|\mathbf{S}| = 1$  spins ruled by a fully connected Heisenberg hamiltonian with an inhomogeneous antiferromagnetic super-exchange coupling  $J(d_{ij}) = J_0 e^{-\alpha d_{ij}}$  where  $J_0$  is the antiferromagnetic nearest neighbour interaction. The  $\alpha$  parameter scales the range of the interaction: as  $\alpha$  decreases the interaction becomes long range. The exchange interaction function  $J(d_{ij})$  can be tuned from ab initio calculation or experimental results [14, 17, 18]. The lattice deformation is constrained by a Lennard-Jones (LJ) potential with a normalised unit distance ( $d_0 = 1$ ). We use extended Monte Carlo Metropolis calculations with both spins and ionic displacements update [17–20]. The competition between the Heisenberg term and the Lennard-Jones potential, respectively tuned by  $\alpha$  and  $K$  parameters introduced in Eq.(1), stabilizes three different ground state structures (Fig.1): simple cubic (SC), body-centered cubic (BCC) and hexagonal close packed (HCP). These structures are obtained either if the system optimizes the super-exchange potential or the

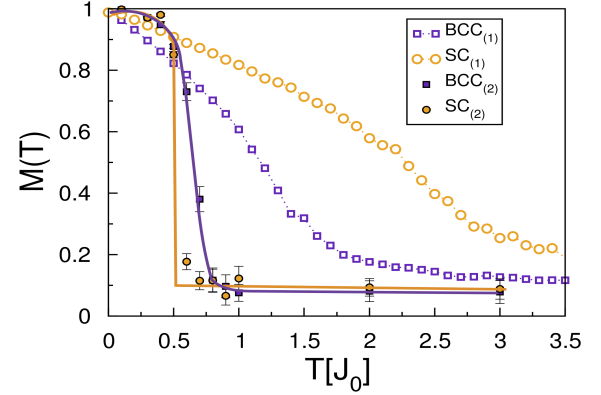


Figure 2: (colors online) Temperature dependent behavior of the magnetic order parameter obtained running equilibrium simulations with (sim<sub>(2)</sub>) and without (sim<sub>(1)</sub>) considering the coupling of the spins with the lattice deformation. The two structures considered are SC (orange) and BCC (violet).

ionic interactions (LJ). When the dominant contribution to the energy is the exchange term, the structure is SC, with a concomitant lattice compression. Indeed the SC structure accommodates the largest number of non-frustrated antiferromagnetic bonds in 3D. For larger  $K$ , we obtain a competition between the exchange and LJ terms. This drives a structural transition towards a BCC structure, which increases the coordination number, albeit retaining an ordered spin structure with pitch vector ( $\mathbf{q} = (0, 0, 2\pi/a)$ ). These two cases show magnetic order (MO). For  $K \gg 1$  the leading contribution comes from the LJ potential, and the system increases further its coordination number losing the magnetic order in favour of the more compact HCP structure. We point out that our case differs from the structural relaxation of Lennard-Jones clusters with zero spins which has been widely studied [21]. Indeed, although the structure is not magnetically ordered, there is a local magnetic optimization which introduces corrections to the energetics. To summarize, we note that the spin-exchange and Lennard-Jones terms are competing in a non trivial fashion in presence of antiferromagnetic interaction: on the one hand, the Lennard-Jones term favors the most compact structure, e.g. the HCP, albeit this phase is magnetically frustrated, and on the other hand the optimal phase to accommodate anti-ferromagnetism in 3D is the regular cubic lattice. This leads to a very rich phase diagram at zero temperature, as mentioned above, but also induces non-trivial effects at finite temperature. We now turn to finite temperature calculations. We first investigate the magnetic phase diagram of the structures with zero temperature magnetic order, obtained in Fig.1 in absence of the ionic motion. In Fig.2 we report the

temperature dependent magnetic order parameter. The magnetic order parameter of the SC phase ( $SC_{(1)}$ ) is stable until  $T \approx 3 [J_0]$ , whereas for frustrated BCC phase ( $BCC_{(1)}$ ) we find a less stable magnetic phase (magnetic for  $T < 1.8 [J_0]$ ). However, once both the spin and ionic potential are considered ( $SC_{(2)}$ ,  $BCC_{(2)}$ ), we observed that both structures are magnetic for  $T < 0.6 [J_0]$ , but the processes leading to the paramagnetic phase are very different. For the SC phase, we observe that the drop of magnetization is concomitant with a loss of the structural properties, as the lattice starts melting at  $T \approx 0.6 [J_0]$ , whereas the BCC structure survives above this temperature, and undergoes a magnetic transition towards the paramagnetic phase due to magnetic fluctuations (further details are included in suppl. mat. Fig.1).

*Dynamical response to a ferromagnetic quench* As we observed that the structural properties are conserved at low enough temperature, we now want to turn the discussion to the dynamical magnetic properties of the nano-structures stabilized so far at equilibrium, by running spin dynamics simulations. The Landau-Lifshitz-Gilbert (LLG) equation has been numerically solved by replacing the spin operators of the Heisenberg Hamiltonian with classical angular momentum vectors. The evolution of each spin can be seen as its precession around an effective field  $\Omega_i = -\sum_{j \neq i} J_{ij} \mathbf{S}_j$  induced by the neighbouring spins. Furthermore, to induce energy dissipation, the system is physically embedded by a thermal bath at constant temperature, mathematically represented by a stochastic field and a dissipative term in the equation. The differential equation of motion reads

$$\frac{d\mathbf{S}_i}{dt} = \frac{1}{\hbar} [\mathbf{S}_i \times (-\Omega_i + \mathbf{h}_i) - \gamma \mathbf{S}_i \times (\mathbf{S}_i \times (-\Omega_i))] \quad (2)$$

where  $\mathbf{h}_i$  a Gaussian distributed white noise with zero mean and vanishing correlator  $\langle h_i(t)h_j(t') \rangle = \mu \delta_{i,j} \delta(t, t')$ , representing the stochastic field. Its value at each time step  $\Delta t$  is  $h_{\alpha,i} = \eta \sqrt{\mu/\Delta t}$  with  $\alpha \in \{x, y, z\}$  being the cartesian coordinate and  $i$  referring to the site label,  $\eta \sim \mathcal{N}(0, 1)$  is a random variable sampled from the standard normal distribution.  $\gamma$  is the Gilbert dissipation parameter related to the stochastic field through the fluctuation dissipation theorem (FDT) [22, 23]  $\mu = 2\gamma k_B T$  at equilibrium. We point out that  $\gamma$  is a dimensionless parameter that can be extracted directly from the spin dynamics simulation or by comparison with Monte Carlo calculations at equilibrium. We found that both are consistent within the error bars (suppl. mat. Fig.2). Note that however the stochastic LLG formalism is valid irrespective by equilibrium or out of equilibrium conditions. The dynamics is implemented via the Suzuki-Trotter decomposition outlined in Ref.[24, 25] and time units have been fixed assuming the exchange interaction being of the typical order of magnitude of the bulk  $J = 0.1$  eV.

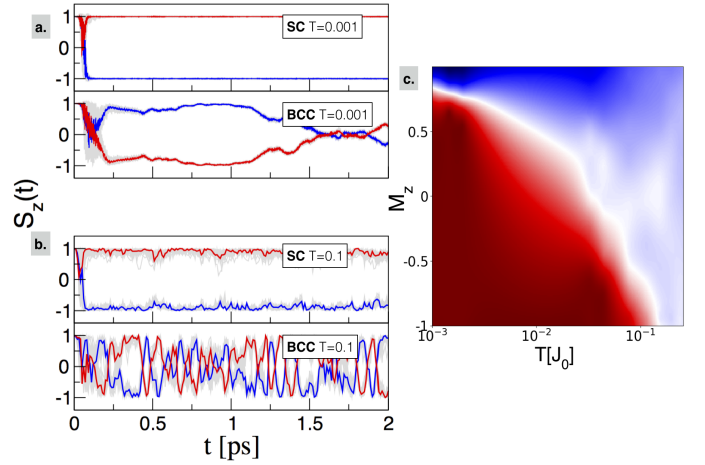


Figure 3: a-b) Time evolution of the z-component  $S_z(t)$  of all the spins (grey solid lines) in the system initially subjected to a ferromagnetic quench: blue and red solid line refer to two sites having opposite magnetic moments after the transient. Results are shown for  $T = 0.001, 0.1 [J_0]$  (top to bottom) respectively for SC and BCC. c) Thermal stability of the polarization of the staggered magnetic vector in terms of  $P(M_z)$ . The color map goes from zero (red) to one (blue). Dynamics considered up to  $t_f = 12$  ps.

### Spin dynamics after a ferromagnetic quench

Since we are interested in the response of the system to an initial out of equilibrium condition, we start from the ferromagnetic configuration and we let the system evolve with the exponential time evolution operator for the spins given by Eq.(1), considering the Born-Oppenheimer approximation where the ions are frozen. At low temperature ( $T = 0.001 [J_0]$ , Fig.3 (a)) the central site of the nanostructures (blue solid line for SC and red for BCC) anti-aligns with respect to its initial configuration along the z-direction under the effect of the evolution operator. The response of the lattice to this mechanism is prompt. Indeed the flipping mechanism diffuses from the core spin to the surface ones (Suppl Mat Fig.S3 (c)-(d)) and the evolution of all spins is synchronized toward the relaxation to the AF state by keeping a global orientation on each of the sublattice. Red and blue lines in Fig.3 (a)-(b) represent the evolution of the z-component of two spins belonging respectively to the ferromagnetic sublattices A and B. The time dependence of the local vector on each site is also shown via the grey dashed area and shows that the time dynamics is synchronous. We note however that, differently from the BCC, at  $T = 0.0001 [J_0]$  (Fig.3 (a)) in the SC only one sublattice is evolving under the time evolution operator, while the other is not affected by the dynamics, and the orientation of the initially applied ferromagnetic field  $\mathbf{B}$  is kept (red solid line). This non-

trivial and interesting dynamics is triggered by the exchange coupling between the sublattices in the AF phase when the system is initially prepared out of equilibrium. The spontaneous locked polarization of the magnetisation in the SC is due to its intrinsic weak ferromagnetic component. Indeed, even if both SC and BCC are able to stabilize a Néel order along all the directions, they differ for the number of uncompensated spins (10% SC and 0.1% BCC). Thus while for BCC the flipping mechanism has  $\approx 2$  ps time scale, the long time dynamics reveals that for the SC it happens at  $t \approx 0.4$  ns for fixed  $T = 0.001[J_0]$  (See Fig.S6 (a) Suppl Mat). We now turn to the discussion of the time evolution at higher temperatures  $T = 0.1[J_0]$  (Fig.3 b) where the systems are still magnetic. We observe that while for the BCC ergodicity is recovered, for SC the obtained time evolution is similar to the  $T = 0.001[J_0]$  case with thermally activated small oscillations around the initial quenching field direction  $\mathbf{B}$ . The picture shown so far for short time window ( $t_f=2$  ps) is extended for longer time simulations ( $t_f=12$  ps) and Fig.3 (c) shows the thermal stability of the polarization of the staggered magnetic vector in terms of  $P(M_z)$ . We hence observe in the SC long-lived non-thermal states, which are non-trivial topologically protected states driven by the interplay of the initial quench and long-range interactions. On the other hand in the BCC, whose structure is not bipartite, the intrinsic magnetic anisotropy due to the geometry does not stabilize a long-lived memory effect against thermal fluctuation.

**Adding a static field** Interestingly, time translational symmetry observed in the transient in Fig.3 (a) is explicitly broken when an applied magnetic field  $\mathbf{h} \rightarrow \tilde{\mathbf{h}} = \mathbf{h} + h_{\text{ext}}[1, 1, 1]$ , pointing along a different direction from the quenched field, is switched on (Eq. [2]) after the ferromagnetic quench. Indeed the spin dynamics after the quench, and upon an applied field, shows a periodic behaviour. Here we consider a small external field ( $h_{\text{ext}} = 0.01, 0.1$ ) and we observe the dynamics in the temperature regime where the effects of the small field are not washed away by thermal fluctuations. Fig.4 (a) shows that while for the BCC the staggered magnetic vector stabilizes along the direction of the field, in the SC the dynamics is characterized by long-lived oscillations and the alignment is recovered at  $t = 20$  ps for  $T = 0.001[J_0]$ ,  $h_{\text{ext}} = 0.1$  (Fig.S6 (b) suppl. mat.). Thus in the SC the spin dynamics after the quench is characterized by two time scales. Firstly at the femtosecond level the antiferromagnetic interaction brings the system toward its energy minimum (from a F to AF configuration): the spins after the ferromagnetic quench follow the same relaxation as in absence of applied field at first, and form an AF state. Secondly at larger time scale the AF state symmetry is maintained and the spins precess around the (1,1,1) direction: this

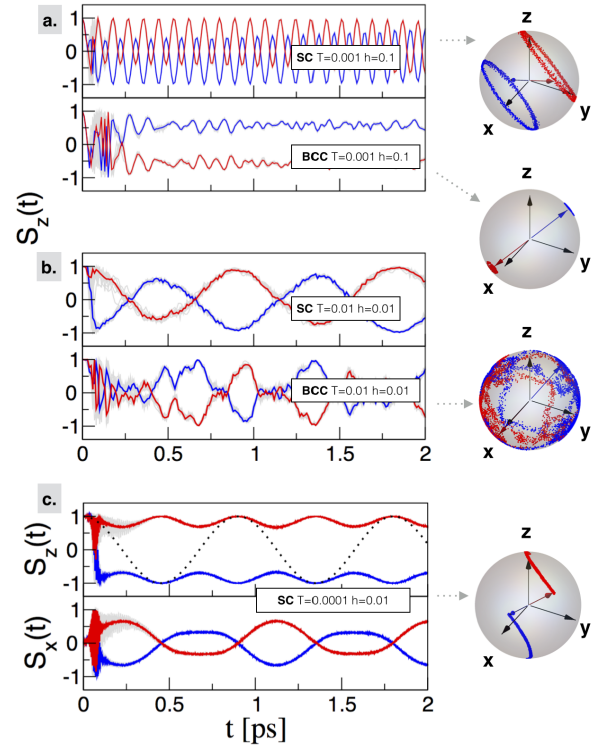


Figure 4: a-b) Time evolution of the z-component  $S_z(t)$  of all the spins (grey solid lines) in the system initially subjected to a ferromagnetic quench at  $t = 0$  and a static field for  $t > 0$ . Blue and red solid line refer to two sites having opposite magnetic moments after the transient. Results are shown for different temperatures and values of the fields (top to bottom) respectively for SC and BCC. c) Time evolution of the x and z-component of the spins  $S(t)$  in the system initially subjected to a ferromagnetic quench at  $t = 0$  and an AC field for  $t > 0$ . The black dashed line refer to the applied AC field  $\cos(2\pi\omega t)$ . Bloch sphere representation of the spin configuration on two different sites (blue and red) having opposite magnetic moments in the steady state.

not trivial dynamics which brings the system towards the alignment along the direction of the external field is characterized by observable timescale (Fig.S6 (b) For  $h_{\text{ext}} = 0.01$  and  $T = 0.0001[J_0]$  the alignment is recovered at  $t = 2$  ns.) The arising of this intermediate phase between the AF stabilization and the alignment with the external field, characterized by a periodic response of the system to a static field, is exclusively triggered by the uncompensated spins in the AF nanocluster. The scenario at  $T = 0.01$  and  $h_{\text{ext}} = 0.01$  (Fig.4b) shows that the periodic phase is even stronger for higher temperature and smaller field than the effect of the field itself: indeed while in the BCC the thermal fluctuations destroyed the effect of  $\mathbf{h}_{\text{ext}}$  in the SC the periodic oscillations are still evident. Thus we discover

an interesting phase of the transient triggered by the AF interactions in a finite system where the response of the system to a static field shows a periodic behaviour. Its relaxation time scale can be observed, tuned and extended.

**Adding an AC field** The last question we want to address concerns the response of the SC system to an AC field  $\mathbf{h} \rightarrow \tilde{\mathbf{h}} = \mathbf{h} + h_{\text{ext}} \cos(2\pi\omega t)[1, 1, 1]$ . Fig.4 (c) shows a peculiar dynamics of the spins in the SC structure: indeed even if the field is applied isotropically, the system shows anisotropic periodic response. In particular the  $s_z$  component of the spins oscillates with half of the period of the applied field, differently from the  $s_{x,y}$  which retain the natural frequency. Thus, the initial ferromagnetic quench and the oscillating applied field prevents the spins from completing a full precession, and instead the covered phase space is limited to a portion of the AF precession circles (see Fig.4 (c)). The spin trajectories explicitly break the time invariance observed in Fig.3 (a), and enter into a periodic motion that lasts beyond the largest time considered in our calculations ( $\approx 1$  ns, Fig.S6 d). This non-trivial time translational symmetry breaking, which protects the  $\mathbb{Z}_2$  topology of the spin trajectories for macroscopic time scales, bears similarities with the recently time crystal observed experimentally in magnetic systems (Ref [5] ). In our calculations, the time-crystal phase (TC) stems from non-thermal states triggered by the non-trivial dynamics obtained after the quench, when, at  $T=0.0001$ , only one of the bipartite sub-lattice evolves with time, whereas the other sub-lattice stays aligned with the applied magnetic field  $\mathbf{B} = (0, 0, 1)$ , and remain topologically protected upon application of AC field. At finite but small temperatures this dynamics breaks the time translational invariance and the spherical symmetry of the spins and in turn provides a nanoscopic time crystal with the magnetic vector aligned along a preferred orientation (induced by a combination of the initial quench and applied magnetic field). In the time crystal phase we observe non thermal states and violation of the FDT (Fig.S4 (a)). At large enough temperature, we recover a relaxation in thermalized states up to  $T = 1$  [ $J_0$ ] (AF phase). For higher temperatures the system is toward its paramagnetic state and the spins lose their synchronous dynamics (PM phase).

**Conclusions** In conclusion we provide results of the role of the spin-lattice coupling in the equilibration of antiferromagnetic nanoscopic system, both at zero and finite temperature. We then focus on the spins quenched dynamics in a temperature regime which foregoes the melting of the magnetic moment. We demonstrate slow relaxation and non-ergodicity in non-disordered nanoscopic many-body systems induced by the initial magnetic quench. The non-thermal states persist in the presence of experimentally controllable classical thermal noise and the signatures of metastability are uncovered in

situations where non-ergodicity is only transient due to dissipation. We develop experimentally accessible witnesses and measures of the breaking of the ergodicity, via the correlation of the order parameter and thus the magnetic relaxivities, which enable future experiments to characterize through observations the properties of non-equilibrium phases of quantum matter. Our work lays out foundations for future experiments in small antiferromagnetic nanoparticles. In particular, for antiferromagnetic SC structures such as perovskites (e.g.  $\text{LaTiO}_3$  [26]) and BCC, widely represented by binary compounds such as  $\text{MnO}_2$ ,  $\text{CuO}$ . Furthermore it provides numerical results for future realization of antiferromagnetic memory devices where magnetocrystalline anisotropy [8] and tunability of the exchange coupling [27] play a crucial role.

*Acknowledgment* We gratefully acknowledge insightful discussions with S.L. Dudarev and P.-W. Ma. C.L. is supported by the EPSRC Centre for Doctoral Training in Cross-Disciplinary Approaches to Non-Equilibrium Systems (CANES, EP/L015854/1). C.W. gratefully acknowledges the support of NVIDIA Corporation , ARCHER UK National Supercomputing Service. We are grateful to the UK Materials and Molecular Modelling Hub for computational resources, which is partially funded by EPSRC (EP/P020194/1).

---

- [1] M. Srednicki. *Phys. Rev. E*, 50:888, 1994.
- [2] M. Rigol, et al. *Nature*, 452:854 EP , 2008.
- [3] J. P. Garrahan. *Physica A: Statistical Mechanics and its Applications*, 2018.
- [4] A. C. Potter, et al. *Phys. Rev. X*, 6:041001, 2016.
- [5] J. Zhang, et al. *Nature*, 543:217 EP , 2017.
- [6] K. Sacha, et al. *Reports on Progress in Physics*, 81(1):016401, 2018.
- [7] S. Yan, et al. *Science Advances*, 3(5), 2017.
- [8] S. Loth, et al. *Science*, 335(6065):196, 2012.
- [9] J.-Y. Bigot, et al. *Nature Physics*, 5:515 EP , 2009.
- [10] V. Baltz, et al. *Rev. Mod. Phys.*, 90:015005, 2018.
- [11] M. Vasilakaki, et al. *Scientific Reports*, 5:9609 EP , 2015.
- [12] K. Chen, et al. *Phys. Rev. B*, 48:3249, 1993.
- [13] C. Holm et al. *Phys. Rev. B*, 48:936, 1993.
- [14] P.-W. Ma, et al. *Phys. Rev. B*, 96:094418, 2017.
- [15] J. Tranchida, et al. *Journal of Computational Physics*, 2018.
- [16] W. F. Brown. *Phys. Rev.*, 130:1677, 1963.
- [17] C. Weber, et al. *Phys. Rev. B*, 72:024449, 2005.
- [18] C. Weber, et al. *Phys. Rev. Lett.*, 91:177202, 2003.
- [19] J. A. Olive, et al. *Phys. Rev. B*, 34:6341, 1986.
- [20] Y. Miyatake, et al. *Journal of Physics C: Solid State Physics*, 19(14):2539, 1986.
- [21] D. J. Wales et al. *The Journal of Physical Chemistry A*, 101(28):5111, 1997.
- [22] S. Chandrasekhar. *Rev. Mod. Phys.*, 15:1, 1943.
- [23] R. Kubo. *Reports on Progress in Physics*, 29(1):255, 1966.
- [24] P.-W. Ma, et al. *Phys. Rev. E*, 82:031111, 2010.

- [25] P.-W. Ma et al. *Phys. Rev. B*, 83:134418, 2011.
- [26] F. El-Mellouhi, et al. *Phys. Rev. B*, 87:035107, 2013.
- [27] J. C. Oberg, et al. *Nature Nanotechnology*, 9:64 EP , 2013.

**Supplementary Material for  
“Nanoscopic time crystal obtained by non-ergodic spin dynamics”**

Carla Lupo and Cedric Weber

**Monte Carlo simulation: melting and demagnetization trade off**

We provide here the complete picture related to the competition between the spin-exchange and Lennard-Jones terms at finite temperature. We investigate the magnetic phase diagram of the structures with zero temperature magnetic order, simple cubic SC and body centered cubic BCC, obtained from the relaxation process at  $T = 0$ . As reported in the main text, in absence of the ionic motion, the magnetic order parameter (Fig.1) of the SC phase ( $SC_{(1)}$ ) is stable until  $T \approx 3 [J_0]$ , whereas for frustrated BCC phase ( $BCC_{(1)}$ ) we find a less stable magnetic phase (magnetic for  $T < 1.8 [J_0]$ ). However, once both the spin and ionic potential are considered ( $SC_{(2)}$ ,  $BCC_{(2)}$ ), we observed that both structures are magnetic for  $T < 0.6 [J_0]$ , but the process leading to the paramagnetic phase are very different. For the SC phase, we observe that the drop of magnetization is concomitant with a loss of the structural properties, as the lattice starts melting at  $T \approx 0.6 [J_0]$  (as shown in the left side panel), whereas the BCC structure survives above this temperature (top panel), and undergoes a magnetic transition towards the paramagnetic phase due to magnetic fluctuations.

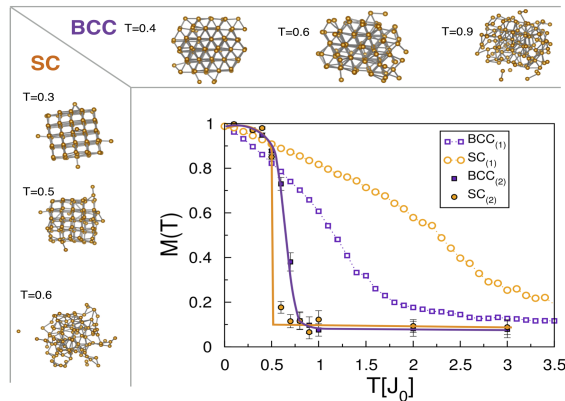


Figure S1: (colors online) Temperature dependent behavior of the magnetic order parameter obtained running equilibrium simulations with ( $sim_{(2)}$ ) and without ( $sim_{(1)}$ ) considering the coupling of the spins with the lattice deformation. The two structures considered are SC (orange) and BCC (violet). Top and left panels show the structures obtained at finite temperature.

**Spin Dynamics simulation**

**Benchmark of stochastic time dependent calculations against Monte Carlo simulations**

Insights on the dynamical magnetic properties of the nano-structures stabilized so far at equilibrium, are obtained by running spin dynamics simulations. The Landau-Lifshitz-Gilbert (LLG) equation [S1] has been numerically solved by replacing the spin operators of the Heisenberg Hamiltonian with classical angular momentum vectors. The evolution of each spin can be seen as its precession around an effective field  $\Omega_i = -\sum_{j \neq i} J_{ij} \mathbf{S}_j$  induced by the neighbouring spins. Furthermore, to induce energy dissipation, the system is physically embedded by a thermal bath at constant temperature, mathematically represented by a stochastic field and a dissipative term in the equation. The differential equation of motion reads

$$\frac{d\mathbf{S}_i}{dt} = \frac{1}{\hbar} [\mathbf{S}_i \times (-\Omega_i + \mathbf{h}_i) - \gamma \mathbf{S}_i \times (\mathbf{S}_i \times (-\Omega_i))] \quad (3)$$

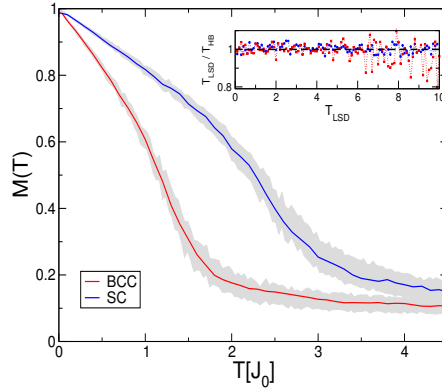


Figure S2: Magnetic order parameter in function of temperature obtained for two different systems (Simple Cubic (SC) in blue and Body Centered Cubic (BCC) in red). The grey shaded regions represent the Langevin statistics. The inset shows the match between the temperature obtained with the *Langevin Spin Dynamics (LSD)* and the Monte Carlo *heatbath* result.

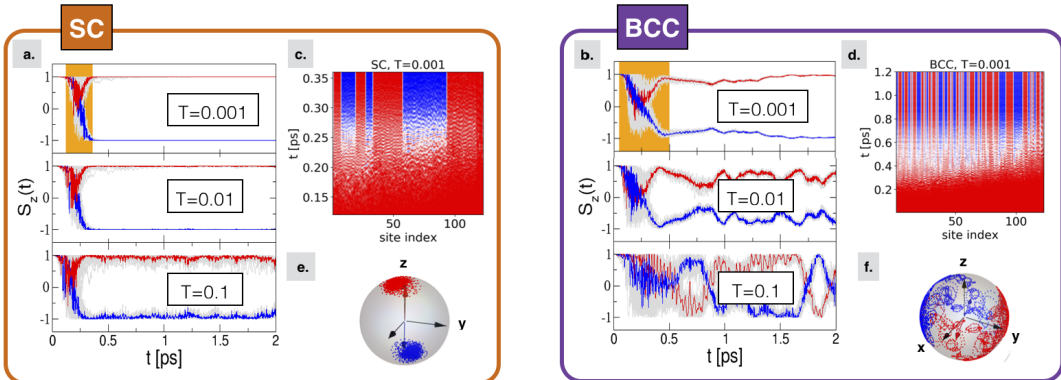


Figure S3: a-b) Time evolution of the z-component  $S_z(t)$  of all the spins (grey solid lines) in the system initially subjected to a ferromagnetic quench: blue and red solid line refer to two sites having opposite magnetic moments after the transient (orange shaded region). Results are shown for  $T = 0.001, 0.01, 0.1 [J_0]$  (top to bottom) respectively for SC and BCC (left to right). c-d) Details of the flipping mechanism during the transient at  $T = 0.001 [J_0]$ , which starts from the central site toward the surface. Sites are labelled according to their distance from the centre. e-f) Bloch sphere representation of the spin configuration at  $T = 0.1 [J_0]$  on two different sites (blue and red) having opposite magnetic moments in the steady state.

where  $\mathbf{h}_i$  a Gaussian distributed white noise with zero mean and vanishing correlator  $\langle h_i(t)h_j(t') \rangle = \mu\delta_{i,j}\delta(t,t')$ , representing the stochastic field. Its value at each time step  $\Delta t$  is  $h_{\alpha,i} = \eta\sqrt{\mu/\Delta t}$  with  $\alpha = (x, y, z)$  being the cartesian coordinate and  $i$  referring to the site label,  $\eta \in \mathcal{N}(0, 1)$  is a random variable sampled from the standard normal distribution.  $\gamma$  is the Gilbert dissipation parameter related to the stochastic field through the fluctuation dissipation theorem (FDT) [S2, S3]  $\mu = 2\gamma k_B T$  at equilibrium. We point out that  $\gamma$  is a dimensionless parameter that can be extracted directly from the spin dynamics simulation or by comparison with Monte Carlo calculations at equilibrium. In Fig.2, we show the magnetic order parameter obtained with *heatbath* simulations and the spin dynamics. Thus the temperature obtained under the hypothesis that FDT is satisfied during the dynamics of the spins [S4] can also be obtained by the equilibrium Monte Carlo simulation.

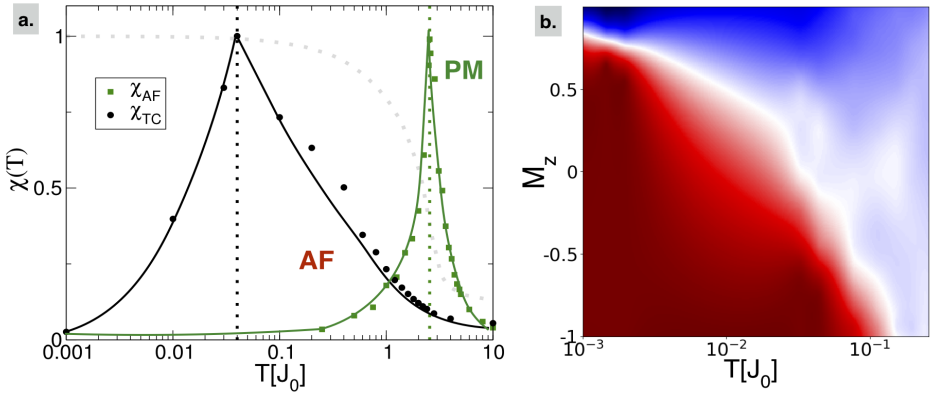


Figure S4: a.) Temperature dependent behaviour of the fluctuations of the order parameter both along the time evolution after the quench (black circles) and at the equilibrium one (green squares). The plot highlights the arising of three different regions: time crystal (TC), magnetically ordered phase (antiferromagnetic AF) and the paramagnetic phase (PM). The structure in analysis is the SC. The grey dashed line is square of the staggered magnetic order parameter. b) Thermal stability of the polarization of the staggered magnetic vector in terms of  $P(M_z)$  in the SC structure. The color map goes from zero (red) to one (blue). Dynamics considered up to  $t_f = 12$  ps and multiple run with same quenched initial conditions.

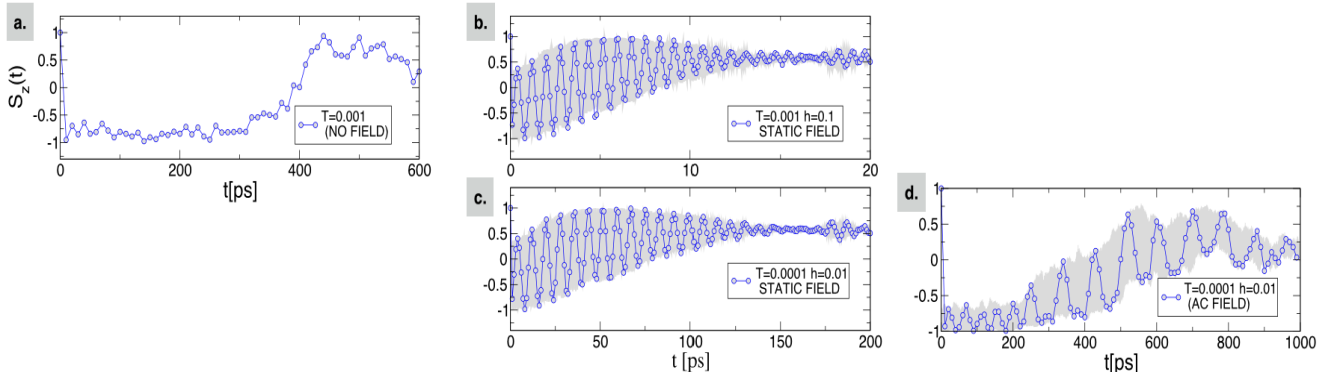


Figure S5: a) Time evolution of the z-component  $S_z(t)$  of the core spin (blue dotted line) in the antiferromagnetic SC subjected to three different protocols. a) System initially ( $t = 0$ ) subjected to a ferromagnetic quench and subsequently let to evolve in absence of any external drive (long time dynamics of Fig.3 (a) in the main text); b-c) Ferromagnetic quench ( $t=0$ ) and a static field  $h = h_{\text{ext}}[1, 1, 1]$  at  $t > 0$  (long time dynamics of Fig.4 (a) in the main text) and d) Ferromagnetic quench ( $t = 0$ ) and an AC field  $h = h_{\text{ext}} \cos(\omega t)[1, 1, 1]$  (long time dynamics of Fig.4 (c) in the main text). Results are shown for different temperatures and  $h_{\text{ext}}$  values.

### Insights on the spin dynamics results

We now want to look at the average quantities which characterize the dynamics of the structures considered and we use the fluctuation dissipation theorem (FDT) to search for the evidence of the non-thermal states observed above. In the following analysis we focus on the SC for which, due to its bipartite structure, the memory effect is enhanced and resistant against thermal fluctuation even in absence of magnetic anisotropy.

In Fig.S4 (a) we calculate both the correlation of the order parameter along the time evolution after the quench and its fluctuations at equilibrium as  $\chi_{\mathbf{q}=\text{AF}}(T)$  (where the wave vector dependent magnetization  $M_{\mathbf{q}} = (1/N) \sum_i \mathbf{S}_i e^{i\mathbf{q} \cdot \mathbf{r}_i}$  has  $\mathbf{q}$  corresponding to ordering wavevector defined for the bulk antiferromagnetic states  $\mathbf{q} = (\pi, \pi, \pi)/a$  for SC). At equilibrium, the two quantities are related by the FDT. However out-of-equilibrium, in a case of a non-ergodic dynamics, a violation of the FDT theorem can be observed for non thermal state. We observe indeed in our calculations

the presence of long-lived non-thermal states obtained after the quench, violating the FDT, at temperature  $T < 0.01 [J_0]$  for SC (and  $T < 0.0001 [J_0]$  for BCC). We hence found three different phases: i) non ergodic but magnetic (TC), ii) ergodic and magnetic (AF) and iii) paramagnetic (PM).

#### Supplementary references

- [S1] W.F. Brown, *Phys. Rev.*, 130:1677, 1963.
- [S2] S.Chandrasekhar, *Rev. Mod. Phys.*, 15:1, 1943.
- [S3] R. Kubo, *Reports on Progress in Physics*, 29(1):255, 1966.
- [S4] P.-W. Ma, et al., *Phys. Rev. E*, 82:031111, 2010.